

Steady and non-steady state magma chambers below the East Pacific Rise

Rodey Batiza¹, Y. Niu², J.L. Karsten¹, W. Boger¹, E. Potts³, L. Norby¹,
and R. Butler⁴

Abstract. Volcanic rocks collected on flowline traverses on the flanks of the East Pacific Rise (EPR) document changes in axial magma chemistry with time, providing a record of the thermal history of axial magma chambers (AMC). We present data for a sample set of closely spaced (1-2 km) samples along EPR flowlines at three localities out to ~800 ka showing both steady (constant average temperature) and non-steady state behavior of magma chambers on time scales of 200-500 ka. Though based on only three symmetrical traverses so far, it appears that magmatically robust ridge locations (11°20'N and 9°30'N) have steady state chambers, whereas a magmatically starved axis (10°30'N) shows large temperature changes with time. These observations provide a new petrologic perspective to the ongoing debate regarding the significance and causes of morphologic variations along the axis of the East Pacific Rise.

Introduction

The petrology of the axis of the global mid-ocean ridge system is relatively well known because of extensive sampling efforts over the last several decades. The large data base of axial "zero-age" volcanic rocks has allowed significant advances in understanding of recent magmatic processes below active ridges (e.g. *Langmuir et al.*, 1992). While the zero-age snapshot is important, temporal variation in the petrogenetic behavior of ridges is also of great interest. Ridges are dynamic features and the history of magmatic processes at single ridge locations is needed for a comprehensive understanding of the dynamic, time-dependent processes of ridge magmatism. For this, off-axis samples from the flanks of mid-ocean ridges are required.

Off-axis samples have been obtained by drilling, dredging, coring, and submersible (e.g. *Aumento*, 1968; *Hekinian*, 1971; *Flower and Robinson*, 1979; *Karsten et al.*, 1990; *Reynolds et al.*, 1992; *Perfit et al.*, 1994). However, systematic off-axis sampling lags far behind sampling of axial lavas and consequently our understanding of the temporal variation of ridge magmatism is at present, highly incomplete.

The purpose of this paper is to present new results of off-axis sampling on the flanks of the EPR. We present evidence for long-term (>200 ka) petrologic temporal variation, interpreted to reflect changes in the average composition and temperature of AMC beneath the axis.

¹Dept. of Geology and Geophysics, SOEST, University of Hawaii and Hawaii Center for Volcanology, Honolulu, Hawaii.

²Dept. of Earth Sciences, University of Queensland, Brisbane, Australia.

³Dept. of Geology, College of Wooster, Wooster, Ohio.

⁴IRIS, Arlington, Virginia.

Copyright 1996 by the American Geophysical Union.

Paper number 95GL00016

0094-8534/96/95GL-00016\$03.00

Results

During Phoenix, leg 2 (*R/V Melville*), samples were collected by dredging and rock coring along flowlines (± 1 km) of the EPR axis at 9°30'N, 10°30'N, and 11°20'N on both the Cocos and Pacific plates out to 40-50 km from the axis, or ~800 ka (*Carbotte and Macdonald*, 1992; *Perram and Macdonald*, 1990; *Duncan and Hogan*, 1994). Figure 1 shows the locations of dredged samples (well-determined by GPS and multibeam bathymetry) taken at an average spacing of ~1.6 km on crust free of seamounts, migrating offset trails and other anomalies. Most dredges were of small fault scarps and recovered talus derived from up to 100-200 m of section. Dredging was 98% successful, indicating that off-axis sampling is feasible even on old, sediment-covered ocean crust.

We obtained major element analyses by electron microprobe for over 550 individual numbered samples and INAA trace elements for ~100 of these. Table 1 gives representative analyses. Figure 2 shows plots of MgO vs. distance from the EPR axis and the distribution of incompatible element-depleted mid-ocean ridge basalt (NMORB) and enriched T and EMORB for each of the three transects and axis. These portions of the EPR were studied previously by *Langmuir et al.*, 1986; *Thompson et al.*, 1989; *Perfit et al.*, 1994; *Batiza and Niu*, 1992; *Reynolds et al.*, 1992; *Hekinian et al.*, 1989, and *Barth et al.*, 1994. One interesting result is that the rough proportion of T and EMORB to NMORB at and near the axis at each locality has apparently remained the same over the last 0.8 ma: a large proportion of EMORB at 11°20'N, a much smaller proportion at 9°30'N and only NMORB at 10°30'N.

The NMORB samples at all three localities display highly symmetrical patterns of MgO variation with distance from the axis. Other major oxides and trace elements display similar patterns, as the chemical variations among samples from each transect are primarily explained by shallow fractionation from either a single parental composition or several parents that are chemically very similar. In addition, there is scatter in the MgO values amounting to ~2-3 wt% variation in MgO at any given sampling site. This variation is about the same or a little greater than variations observed in some restricted areas along the EPR axis and near-axis regions (*Langmuir et al.*, 1986; *Batiza and Niu*, 1992; *Reynolds et al.*, 1992; *Perfit et al.*, 1994), but is smaller than observed at other areas of the EPR such as the 8°37'-9°03'N area and the area just north of the Clipperton transform (*Langmuir et al.*, 1986).

Discussion

In interpreting the broad chemistry vs. distance patterns for the three transects (Fig. 2), we make several assumptions. The first is that our samples are representative of the upper 100-200 m of the volcanic layer of the crust emplaced at or within 1-2 km of the axis and are not systematically biased toward samples erupted farther off-axis. This assumption is reasonable because, despite the finite width of the active axial eruptive zone at the

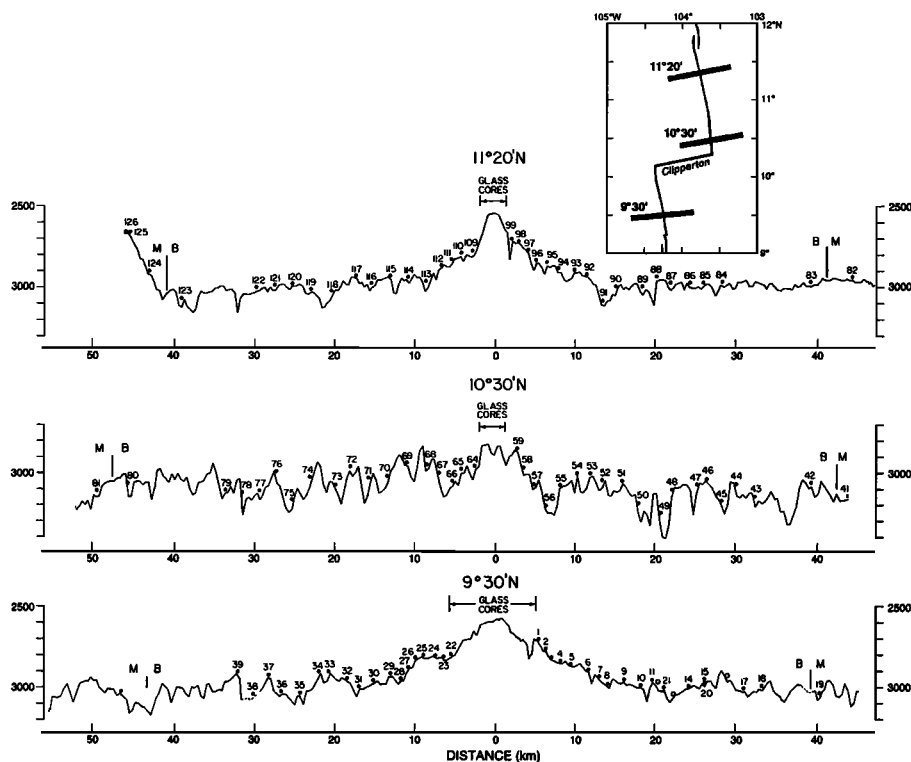


Figure 1. Bathymetric profiles along the three flowline sampling traverses. Dots with numbers are dredge locations and the Bruhnes-Matuyama magnetic boundary (from *Carbotte and Macdonald, 1992* and *Perram and Macdonald, 1990*) are shown. Spreading rates are ~ 110 mm/yr and roughly the same in all three areas. Note that many of the dredges sampled fault scarps. Also note that the two magmatically robust ridge locations ($9^{\circ}30'N$ and $11^{\circ}20'N$) have relatively smooth topography off-axis, whereas the magma starved ridge at $10^{\circ}30'N$ has much rougher topography. The morphologic studies of *Goff* (1991) indicate that these morphologic differences persist for several million years off-axis. This suggests that magma supply and axial morphologic character are relatively long-lived phenomena, as proposed by *Barth et al.*, (1994).

Table 1. Representative glass analyses.

	PH2-3	PH14-1	PH35-3	PH43-2	PH59-2	PH76-1	PH78-2	PH90-2	PH117-6	PH123-2
Area	$9^{\circ}30'N$	$9^{\circ}30'N$	$9^{\circ}30'N$	$10^{\circ}30'N$	$10^{\circ}30'N$	$10^{\circ}30'N$	$10^{\circ}30'N$	$11^{\circ}20'N$	$11^{\circ}20'N$	$11^{\circ}20'N$
Latitude (N)	$9^{\circ}31.05'$	$9^{\circ}31.99'$	$9^{\circ}29.21'$	$10^{\circ}30.91'$	$10^{\circ}29.25'$	$10^{\circ}25.87'$	$10^{\circ}25.60'$	$11^{\circ}22.43'$	$11^{\circ}19.51'$	$11^{\circ}17.82'$
Longitude (W)	$104^{\circ}11.29'$	$104^{\circ}01.55'$	$104^{\circ}27.79'$	$103^{\circ}19.23'$	$103^{\circ}35.04'$	$103^{\circ}49.56'$	$103^{\circ}51.77'$	$103^{\circ}38.32'$	$103^{\circ}55.29'$	$104^{\circ}06.59'$
Depth (m)	2888	2880	2971	3166	2893	3323	3142	3003	2978	3100
Major Elements (wt%)										
SiO ₂	50.22	50.62	51.41	57.56	51.04	50.35	52.72	50.61	50.99	50.78
TiO ₂	2.40	1.30	2.33	2.00	2.61	0.98	3.20	2.15	3.07	1.73
Al ₂ O ₃	14.10	14.99	13.33	12.31	13.76	14.85	12.42	14.97	14.70	14.67
FeO	12.19	9.18	12.85	13.85	12.56	10.07	14.74	10.54	12.56	10.26
MnO	0.20	0.17	0.23	0.27	0.23	0.20	0.26	0.19	0.23	0.21
MgO	5.72	7.71	5.59	1.81	6.01	8.24	3.90	6.17	4.27	7.26
CaO	10.61	12.63	10.27	6.09	10.50	13.14	7.99	10.95	8.94	11.71
Na ₂ O	3.38	2.75	3.15	4.12	2.90	1.81	3.68	3.44	3.77	2.69
K ₂ O	0.43	0.09	0.19	0.72	0.20	0.01	0.38	0.54	1.09	0.13
P ₂ O ₅	0.30	0.10	0.21	0.73	0.24	0.07	0.48	0.33	0.47	0.15
Total	99.56	99.54	99.55	99.46	100.06	99.73	99.76	99.88	100.08	99.61
Trace Elements (ppm)										
Sc	42	42	43	26	42	43	37	42	31	41
Cr	83	393	47	2	136	284	18	143	8	347
Sr	250	110	130	160	150	50	160	250	340	140
Zr	170	150	130	610	170	60	300	180	210	20
La	10.60	2.61	5.78	23.70	5.86	0.67	13.11	10.28	22.00	2.83
Ce	26.10	8.90	16.30	67.50	17.40	2.70	38.40	24.60	48.00	8.90
Sm	5.72	2.77	5.12	17.69	5.40	1.91	10.99	5.14	7.44	2.93
Eu	1.95	1.10	1.78	4.74	1.81	0.81	3.25	1.79	2.39	1.12
Tb	1.19	0.69	1.25	3.83	1.29	0.57	2.51	1.04	1.38	0.79
Yb	4.23	2.51	4.73	14.85	4.96	2.60	9.45	3.67	4.21	2.89
Lu	0.65	0.37	0.70	2.13	0.75	0.39	1.38	0.53	0.63	0.43
Hf	4.53	2.12	4.27	15.70	4.25	1.36	9.22	4.15	6.03	2.13
Ta	0.69	0.11	0.31	1.19	0.33	0.03	0.69	0.81	1.78	0.12
Mg#	48.2	62.5	46.3	20.5	48.7	61.8	34.4	53.7	40.2	58.4
K/Ti	0.25	0.10	0.11	0.50	0.11	0.02	0.16	0.35	0.49	0.10
(La/Sm)N	1.02	0.52	0.62	0.73	0.60	0.19	0.65	1.10	1.62	0.53
Type	T	N	N	N	N	N	T	E	E	N

Major elements were analyzed on glass chips by electron microprobe at Lamont Doherty Earth Observatory. Trace elements were analyzed by instrumental neutron activation analysis (INAA) at Washington University, St. Louis. Analytical uncertainties are given in Batiza and Niu (1992). N-MORB, E-MORB and T-MORB are as defined by Hekinian et al. (1989).

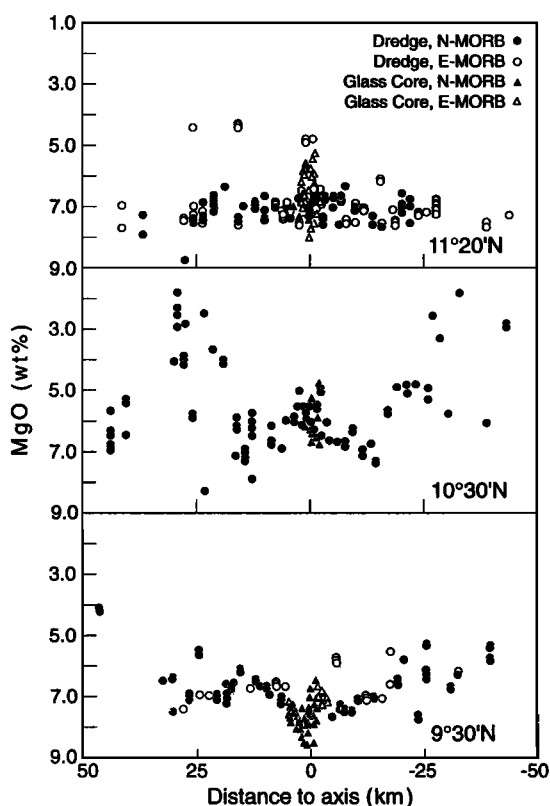


Figure 2. Plots of MgO (wt%) vs. distance from the axis. Negative distances are on the Cocos plate. Note the symmetry of the patterns about the axis, the long wavelength changes in MgO with distance and the range of compositional variation (scatter) both on and off-axis. Note that the proportion of NMORB to EMORB near the axis is grossly the same off-axis at each locality. Near axis data at 9°30'N are from *Perfit et al.* (1994).

EPR at ~9°30'N and the finding of zero-age eruptions up to ~4 km from the axis (*Goldstein et al.*, 1994; *Perfit et al.*, 1994), available evidence indicates that the volume of material erupted farther than 1-2 km from the axis is probably small (*Harding et al.*, 1993; *Macdonald et al.*, 1983; *Carbotte and Macdonald*, 1992; *Perfit et al.*, 1994), though individual flows may be areally extensive. To avoid possible bias from oversampling a thin veneer of eruptions emplaced off-axis at the distal edges of the axial zone, we mostly sampled fault scarps exposing 100-200 m of section.

We secondly assume that the patterns of Figure 2 are unaffected by signal aliasing as might occur by undersampling a high (chemical)-amplitude signal of wavelength shorter than our sample interval of ~1.6 km (~20,000 yrs). This possibility can be ruled out because our sample-spacing is not regular, but varies from 1-3 km depending on the spacing of fault scarps (Fig. 1). More importantly, the symmetry of the patterns argues strongly against aliasing. For this symmetry to have been created as an artifact is highly implausible for a single traverse, much less all three symmetrical profiles.

The observed scatter in MgO values at each locality (Fig. 2) could be due to chemical heterogeneity of the AMC (e.g. *Sinton and Detrick*, 1992), rapid (0.1-1 ka) compositional change of the AMC melt lens (e.g. *Reynolds et al.*, 1992), and/or mixed ages and compositions from an eruptive axis up to several km. wide (*Perfit et al.*, 1994). While we cannot rule out the possibility of a limited range of sample ages at each dredge

locality, the range of chemical variation (scatter) suggests that the range of ages is relatively small and on the same order as observed elsewhere along the EPR at and near the axis (*Langmuir et al.*, 1986; *Batiza and Niu*, 1992; *Reynolds et al.*, 1992; *Perfit et al.*, 1994).

Accordingly, we interpret the chemical variations of Figure 2 as representing a random sample of the temporal record of near-axis eruptions preserved on the EPR flanks at each of the three localities. Since this record is linked to the average composition and temperature of the eruptible portions of the AMC, we can document, for the first time, the average temperature history of these three AMCs for the last ~800 ka. Figure 3 shows smoothed plots of lava eruption temperature, computed from MgO content of glasses using the experimental data of *Bender et al.* (1978), vs. distance from the EPR axis.

At 11°20'N the eruptible portion of the AMC has had an average temperature of $1190^{\circ}\text{C} \pm 25^{\circ}\text{C}$ with no significant temporal change over the last 800 ka. The uncertainty represents a range due to the real chemical variation (scatter) seen in Figure 2. At 9°30'N, the average temperature of the AMC has been $\sim 1180^{\circ}\text{C} \pm 22^{\circ}\text{C}$ with a possible small decrease in the past. While the symmetry of the chemical variations at 9°30'N (Fig. 2) may suggest real variation, the magnitude of the chemical change is at the edge of statistical significance given the data scatter at the axis and along the traverse. The axes at 9°30'N and 11°20'N are broad, shallow and have other geophysical characteristics of robust ridge axes (*Macdonald and Fox*, 1988; *Scheirer and Macdonald*, 1993), including a magma lens reflector (*Detrick et al.*, 1987). Our data show that both these ridge segments have magma chambers that have remained at essentially the same temperature (steady state) for the last ~800 ka.

In contrast, the deep, narrow axis at 10°30'N is magmatically "starved" and lacks a seismic magma lens reflector. Figs. 2 & 3 show that this AMC has had temperature changes of ~160°C over the last 600 ka, from $1220^{\circ}\text{C} \pm 20^{\circ}\text{C}$ to $1060^{\circ}\text{C} \pm 20^{\circ}\text{C}$, indicating significant departures from strict thermal steady state behavior over this period. In addition, Figure 2 shows that there may also be large chemical variations over shorter time scales. These observations are perhaps not surprising, as the correlation between MgO and axial depth and cross-section (*Langmuir et al.*, 1986; *Scheirer and Macdonald*, 1993) shows more

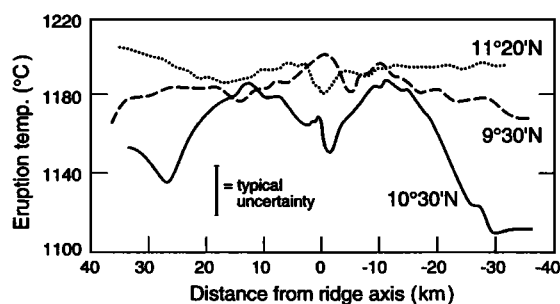


Figure 3. Average eruption temperatures along the three traverses computed from the data of Figure 2. The data were averaged using a moving boxcar 3 km wide and smoothed with a cubic spline. Uncertainties in eruption temperature due to compositional scatter are slightly different for each profile (see text) but are $\pm 25^{\circ}\text{C}$ - 30°C larger than uncertainties in the determination of eruption temperatures ($\pm 10^{\circ}\text{C}$). Note that the two robust ridge locations (9°30'N and 11°20'N) have essentially constant temperatures (thermal steady state) whereas the magma starved ridge at 10°30'N shows significant departures from thermal steady state.

fractionated magmas (on average) occur at deep axes, such as commonly found near offsets (e.g. *Macdonald and Fox*, 1988). Further, it is reasonable that small composite AMCs would be thermally more vulnerable (*Sinton and Detrick*, 1992) and thus subject to larger temperature variation than larger AMCs. While data for other localities are needed to fully test this idea, our data indicate a correlation between axial morphology and AMC thermal history, with robust ridge locations having steady state chambers and starved ridge locations having chambers that depart from steady state.

Acknowledgments. Supported by NSF and ONR. We thank R. Duncan, K. Rubin, J. Sinton, J. Mahoney, and J. Reynolds for helpful input. We also thank the Captain and crew of the *R/V Melville*, K. Macdonald for maps and M. Perfit and D. Fornari for chemical data from their 9°30'N study. We are grateful for the helpful comments of reviewers E. Klein, C. Langmuir, and M. Perfit. This is SOEST Contribution 3981.

References

- Aumento, F., The Mid-Atlantic Ridge near 45°N, II. Basalts from the area of Confederation Peak, *Can. J. Earth Sci.*, **5**, 1-21, 1968.
- Barth, G. A., K. A. Kastens, and E. M. Klein, The origin of bathymetric highs at ridge-transform intersections: A multi-disciplinary case study at the Clipperton Fracture Zone, *Mar. Geophys. Res.*, **16**, 1-50, 1994.
- Batiza, R., and Y. Niu, Petrology and magma chamber processes at the East Pacific Rise ~9°30'N, *J. Geophys. Res.*, **97**, 6779-6797, 1992.
- Bender, J. F., F. N. Hodges, and A. E. Bence, Petrogenesis of basalts from the project FAMOUS area: experimental study from 0 to 15 kbars, *Earth Planet. Sci. Lett.*, **41**, 277-302, 1978.
- Carbotte, S. and K. Macdonald, East Pacific Rise 8°-10°30'N: evolution of ridge segments and discontinuities from SeaMARC II and three-dimensional magnetic studies, *J. Geophys. Res.*, **97**, 6959-6982, 1992.
- Detrick, R. S., P. Buhl, E. Vera, J. Mutter, J. Orcutt, J. Madsen, and T. Brocker, Multichannel seismic imaging of a crustal magma chamber along the East Pacific Rise, *Nature*, **236**, 35-41, 1987.
- Duncan, R. A., and L. G. Hogan, Radiometric dating of young MORB using ⁴⁰Ar-³⁹Ar incremental heating method, *Geophys. Res. Lett.*, **21**, 1927-1930, 1994.
- Flower, M. F. J., and P. T. Robinson, Evolution of the 'FAMOUS' ocean ridge segment: evidence from submarine and deep sea drilling investigations, in *Deep-Drilling Results in the Atlantic Ocean: Ocean Crust*, edited by M. Talwani, C. G. Harrison, and D. E. Hayes, American Geophysical Union, pp. 314-330, 1979.
- Goldstein, S. J., M. R. Perfit, R. Batiza, D. J. Fornari, and M. T. Murrell, Off-axis volcanism at the East Pacific Rise based on U-series dating of basalts, *Nature*, **367**, 157-159, 1994.
- Goff, J. A., A global and regional stochastic analysis of near-ridge abyssal hill morphology, *J. Geophys. Res.*, **96**, 21,713-21,737, 1991.
- Harding, A. J., G. A. Kent, and J. A. Orcutt, A multi-channel seismic investigation of upper crustal structure at 9°N on the East Pacific Rise: Implications for crustal accretion, *J. Geophys. Res.*, **98**, 13,925-13,944, 1993.
- Hekinian, R., Chemical and mineralogical differences between abyssal hill basalts and ridge tholeiites in the eastern Pacific Ocean, *Mar. Geol.*, **11**, 77-91, 1971.
- Hekinian, R., G. Thompson, and D. Bideau, Axial and off-axial heterogeneity of basaltic rocks from the East Pacific Rise at 12°35'N-12°51'N and 11°26'N-11°30'N, *J. Geophys. Res.*, **94**, 17,437-17,464, 1989.
- Karsten, J. L., J. R. Delaney, J. M. Rhodes, and R. A. Lias, Spatial and temporal evolution of magmatic systems beneath the Endeavour segment, Juan de Fuca Ridge: Tectonic and petrologic constraints, *J. Geophys. Res.*, **95**, 19,235-19,256, 1990.
- Langmuir, C. H., J. F. Bender, and R. Batiza, Petrological and tectonic segmentation of the East Pacific Rise, 5°30'-14°30'N, *Nature*, **322**, 422-429, 1986.
- Langmuir, C. H., E. M. Klein, and T. Plank, Petrological systematics of mid-ocean ridge basalts: constraints on melt generation beneath ocean ridges, in *Mantle flow and melt generation at Mid-Ocean Ridges*, edited by J. Phipps Morgan, D. K. Blackman, and J. M. Sinton, *AGU Monograph*, **71**, 183-280, 1992.
- Macdonald, K. C., and P. J. Fox, The axial summit graben and cross-sectional shape of the East Pacific Rise as indicators of axial magma chambers and recent volcanic eruptions, *Earth Planet. Sci. Lett.*, **88**, 119-131, 1988.
- Macdonald, K. C., S. P. Miller, B. P. Luyendyk, T. M. Atwater, and L. Shure, Investigation of a Vine-Matthews magnetic lineation with a submersible; The source character of marine magnetic anomalies, *J. Geophys. Res.*, **88**, 3403-3418, 1983.
- Perfit, M. R., D. J. Fornari, M. C. Smith, J. F. Bender, C. H. Langmuir, R. M. Haymon, Small-scale spatial and temporal variations in mid-ocean ridge crest magmatic processes, *Geology*, **22**, 375-379, 1994.
- Perram, L. J., and K. Macdonald, A one-million year history of the 11°45'N East Pacific Rise discontinuity, *J. Geophys. Res.*, **95**, 21,363-21,381, 1990.
- Reynolds, J. R., C. H. Langmuir, J. F. Bender, K. A. Kastens, and W. B. F. Ryan, Spatial and temporal variability in the geochemistry of basalts from the East Pacific Rise, *Nature*, **359**, 493-499, 1992.
- Scheirer, D. S. and K. C. Macdonald, Variations in cross-sectional area of the axial ridge along the East Pacific Rise: evidence for the magmatic budget of a fast-spreading center, *J. Geophys. Res.*, **98**, 7871-7885, 1993.
- Sinton, J. M., and R. S. Detrick, Mid-ocean ridge magma chambers, *J. Geophys. Res.*, **97**, 197-216, 1992.
- Thompson, G., W. B. Bryan, and S. E. Humphris, Axial volcanism on the East Pacific Rise, 10°-12°N, in *Magnetism in the Ocean Basins*, edited by A. D. Saunders and M. J. Norry, Geol. Soc. Spec. Publ. No. 42., 181-200, 1989.

¹Department of Geology and Geophysics, SOEST, University of Hawaii and Hawaii Center for Volcanology, Honolulu, HI 96822, USA.

²Department of Earth Sciences, University of Queensland, Brisbane, Queensland, 4072, Australia.

³Department of Geology, College of Wooster, Wooster, OH 44691, USA.

⁴IRIS, Suite 1440, 1616 N. Fort Myer Drive, Arlington, VA 22209, USA.